SF2A 2015
F. Martins, S. Boissier, V. Buat, L. Cambrésy and P. Petit (eds)

A NEW 4-D DYNAMICAL MODELLING OF THE MOON ORBITAL AND ROTATIONAL MOTION DEVELOPED AT POLAC

A. Bourgoin[1], C. Le Poncin-Lafitte[1], S. Bouquillon[1], G. Francou[1] and M.-C. Angonin[1,]

Abstract. Nowadays, General Relativity (GR) is very well tested within the Solar System using observables given by the tracking of spacecraft (Bertotti et al. 2003), Very Long Baseline Interferometry (Lambert & Le Poncin-Lafitte 2009, 2011) and Lunar Laser Ranging -LLR- (Merkowitz 2010). These tests are mainly based on two frameworks: the Parametrized Post Newtonian (PPN) and the search for a fifth force. However other frameworks are available and can be used to look for deviations from GR. In this context, we present the ongoing work concerning LLR performed at POLAC (Paris Observatory Lunar Analysis Center) in SYRTE, Paris Observatory. We focus on a new generation of software that simulates the observable (the round trip time of photons) from a given space-time metric (Hees et al. 2012). This flexible approach allows to perform simulations in any alternative metric theories of gravity. The output of these software provides templates of anomalous residuals that should show up in real data if the underlying theory of gravity is not GR. Those templates can be used to give a rough estimation of the constraints on the additional parameters involved in the alternative theory. To succeed, we are building a numerical lunar ephemeris which integrates the differential equations governing the orbital and rotational motion of bodies in the Solar System. In addition, we integrate the difference between the Terrestrial Time (TT) and the Barycentric Dynamical Time (TDB) to make the ephemeris self-consistent. Special attention is paid to the computation of partial derivatives since they are integrated numerically from the variational equations.

Keywords: general relativity, fundamental physics

1 Context

Since 1969 LLR is one of the best tool to constrain GR. However these constraints are generally computed within two frameworks : PPN formalism (Will 1993) and the fifth force framework (Fischbach & Talmadge 1999). Therefore, parameters involved in these two formalism, are very well estimated and point towards GR. For instance, the solution of Williams et al. (2004) yields a numerical test of the equivalence principle with LLR comparable with the present laboratory limit at one part over 10^{13}. It also improved constraints on the strong equivalence principle parameter η (=0 in GR), PPN parameter of non linearity β (=1 in GR), geodetic precession effect and $\dot{G}/G$. Soffel et al. (2008) consider a potential test of the gravitomagnetism effect and the link with the preferred frame parameter α_1 (=0 in GR) appearing in the usual PPN framework. Finally, for the search of a fifth force Müller et al. (2005) performed LLR analysis of the inverse square law by fitting Yukawa perturbation terms.

Most of the time, tests realised in the PPN formalism, are performed in fully-conservative metric theories. However looking for deviations from GR in semi-conservatives, non-conservatives metric theories or even in other phenomenological frameworks like SME (Colladay & Kostelecký 1997, 1998) could be very interesting. Indeed many alternative theories to GR predict for instance a violation of the Lorentz symmetry at different levels. In this attempt, we are building a new numerical lunar ephemeris computed in alternative frameworks to GR and which will be fit on LLR data.

[1] SYRTE, Observatoire de Paris, PSL Research University, CNRS, Sorbonne Universités, UPMC Univ. Paris 06, LNE, 61 avenue de l'observatoire, 75014 Paris, France

2 Main effects

Considering the high accuracy of the LLR data, we have to model all the dynamical effects with theoretical signal larger than 1 cm over the Earth-Moon distance. The most important are (i) the point-mass interactions, (ii) figure potential, (iii) tides and spin deformations of (iv) anelastic bodies and (v) lunar librations.

(i) The numerical integration of the positions of point-mass bodies is done in the International Celestial Reference System (ICRS). We use the post-Newtonian Eistein-Infeld-Hoffmann (EIH) equations of motion in PPN framework, see e.g. Klioner & Soffel (2000). The difference between TT and TDB is also integrated.

(ii) The Moon, the Sun and the Earth are not considered as point-mass bodies. We use spherical harmonics to describe their figure potential. We expand the Earth potential up to degree 4 in zonal harmonic, up to degree 4 in zonal, sectoral and tesseral harmonic for the Moon and only the 2^{nd} degree in zonal harmonic is considered for the Sun.

(iii) We take into account distortions (due to tides and spin variation) raised upon the Earth and the Moon since they are closed to each other. These distortions induce variations in 2^{nd} degree harmonic of the two extended bodies. Subsequently, the impact on the orbital motion of point-mass body is computed with the figure potential formalism described in (ii).

(iv) Distortions are evaluated considering anelastic bodies. Since anelastic bodies don't react immediately to a perturbation, there is a time delay in their reaction because of the dissipation inside them. To consider this dissipation for tides, we introduce a phase lag between the position of a tide raising body and the direction of the tidal bulge. For the spin velocity vector, we consider dissipation by computing the angular velocity vector at time t minus time delay.

(v) We orientate the Moon in ICRS thanks to the three Euler's angles (ϕ, θ, ψ). Their evolution in time is given by Euler's equation of motion which relates the change in Moon angular velocity vector with the Moon total moment inertia tensor and its time derivative. Torques acting on the Moon come from different contributions: (a) interactions of point-mass bodies with the non-spheric potential of the Moon; (b) interaction between the figure of the Earth and the one of the Moon. (c) geodetic precession effect.

3 Partials derivatives

One of the most important specificity of our approach compared to others numerical ephemeris, is the computation of partials from variational equations. In the least squares procedure partials represent the link between the computed and the observed values. We choose to integrate them at the same time than the equations of motion with the ODEX integrator (Hairer et al. 1993). In the standard least squares fit applied to LLR, the new parameters vector $\boldsymbol{x}$ is determined from the initial parameters vector $\boldsymbol{x_0}$ as well as the range measured and the range numerically integrated $f(\boldsymbol{x_0})$. We also need $f'(\boldsymbol{x_0})$ the partial derivative matrix, computed from the variational equations. It depends on initial values of the solution vector : $\boldsymbol{x_0} = {}^{\mathrm{T}}(\rho_1^i, \cdots, \rho_n^i, \zeta^i;\ \dot\rho_1^i, \cdots, \dot\rho_n^i, \dot\zeta^i;\ p^l)$, where $i = 1, \cdots, 3$; $l = 1, \cdots, m$; $\boldsymbol{p}$ being the physical parameters vector, $\boldsymbol{\rho}_{\mathrm{A}}$ the position vector of body A, $\dot{\boldsymbol{\rho}}_{\mathrm{A}}$ the velocity vector of body A, $\boldsymbol{\zeta}$ the three Euler's angles and $\dot{\boldsymbol{\zeta}}$ their time derivatives. Then, for $i = 1, \cdots, 3$, $A = 1, \cdots, n$ and $j = 1, \cdots, 6(n+1)+m$, we integrate the $3n[6(n+1)+m]$ following equations :

$$\begin{cases} \dfrac{\mathrm{d}}{\mathrm{d}t}\left(\dfrac{\mathrm{d}\rho_{\mathrm{A}}^i}{\mathrm{d}x_0^j}\right) = \dfrac{\mathrm{d}\dot\rho_{\mathrm{A}}^i}{\mathrm{d}x_0^j} \\ \dfrac{\mathrm{d}}{\mathrm{d}t}\left(\dfrac{\mathrm{d}\dot\rho_{\mathrm{A}}^i}{\mathrm{d}x_0^j}\right) = \displaystyle\sum_{\mathrm{B},k} \frac{\partial \alpha_{\mathrm{A}}^i}{\partial \rho_{\mathrm{B}}^k}\frac{\mathrm{d}\rho_{\mathrm{B}}^k}{\mathrm{d}x_0^j} + \sum_{\mathrm{B},k} \frac{\partial \alpha_{\mathrm{A}}^i}{\partial \dot\rho_{\mathrm{B}}^k}\frac{\mathrm{d}\dot\rho_{\mathrm{B}}^k}{\mathrm{d}x_0^j} + \sum_{k} \frac{\partial \alpha_{\mathrm{A}}^i}{\partial \zeta^k}\frac{\mathrm{d}\zeta^k}{\mathrm{d}x_0^j} + \sum_{k} \frac{\partial \alpha_{\mathrm{A}}^i}{\partial \dot\zeta^k}\frac{\mathrm{d}\dot\zeta^k}{\mathrm{d}x_0^j} + \frac{\partial \alpha_{\mathrm{A}}^i}{\partial x_0^j}\,, \end{cases}$$

where $\boldsymbol{\alpha}_{\mathrm{A}} = \ddot{\boldsymbol{\rho}}_{\mathrm{A}}(\boldsymbol{x_0})$ is the absolute acceleration vector of body A. We obtain a similar expression for $\mathrm{d}\zeta^i/\mathrm{d}x_0^j$ where $\boldsymbol{\alpha}_{\mathrm{A}}$ is replaced by $\ddot{\boldsymbol{\zeta}}$ the acceleration over the three Euler angles. Partial derivatives in the second member are computed analytically and directly implemented into the software. The numerical integration of the $\mathrm{d}\rho_{\mathrm{A}}^i/\mathrm{d}x_0^j$ quantities let to compute the partial derivatives matrix $f'(\boldsymbol{x_0})$. Using this semi-numerical method, we integrate partials at the same time than the equations of motion unlike a purely numerical method.

4 Comparison with INPOP13c

We present a comparison between our numerical solution and INPOP13c (Fienga et al. 2014). Currently, the two dynamical modelling are closed to each other except three main differences: (a) into our numerical solution, the Earth orientation is forced with the IAU-routines of SOFA (Wallace 1998), whereas it is integrated into INPOP13c; (b) we consider the perturbation upon the Earth-Moon vector of the 70 biggest asteroids, while the effect of 300 is computed into INPOP13c; (c) INPOP13c takes into account a flat ring in order to model the remaining asteroids of the main belt, which is not present in our software.

In Fig. 1, 2 and 3 we compare the two dynamical modelling by taking initial conditions (positions and velocities) of bodies as well as values of physical parameters provided by INPOP13c at J2000. We have integrated the differential equations with our software and plotted the differences between our solution and INPOP13c. In Fig. 1 is shown the difference over the Earth-Moon distance on the left panel and the distribution around the mean value on the right panel. In Fig. 2 is plotted the differences over the 6 Keplerian elements of the Moon, and the three Euler's angles and their time derivatives in Fig. 3.

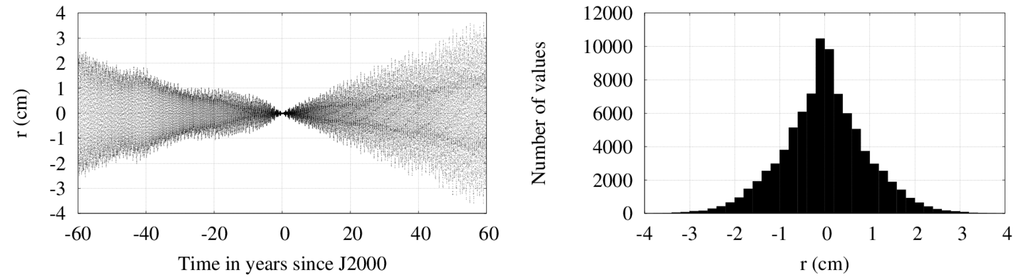

Fig. 1. Left: Difference over the Earth Moon distance after an integration with initial conditions provided by INPOP13c. The x axis is TDB time expressed in years since J2000. **Right:** Distribution of this difference around the mean value.

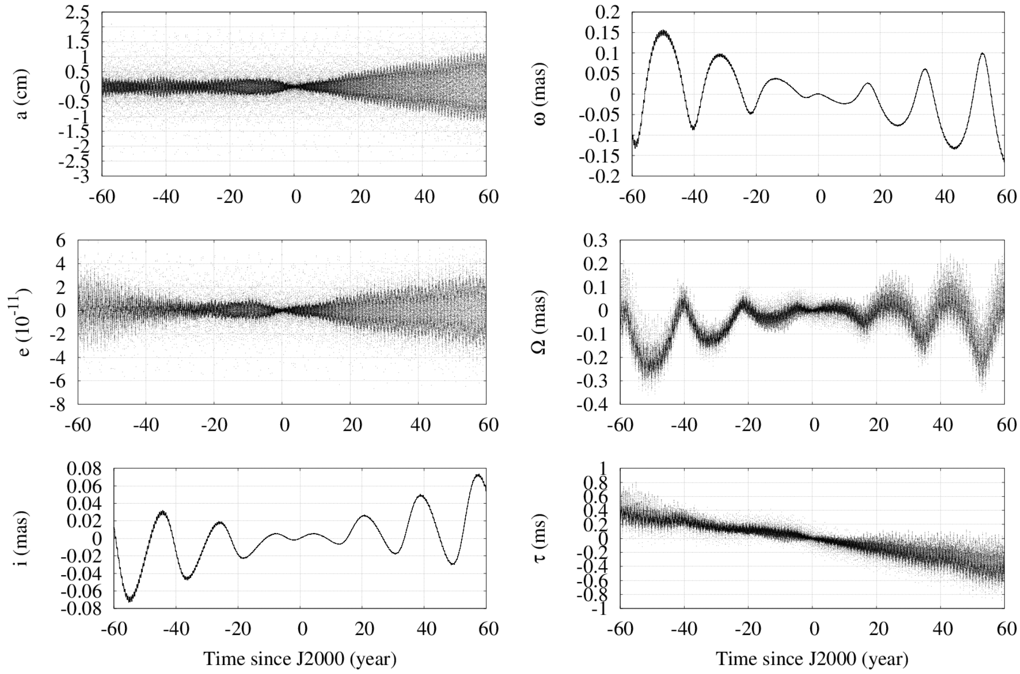

Fig. 2. Differences over the 6 keplerian elements of the Moon after an integration with initial conditions provided by INPOP13c. The x axis is TDB time expressed in years since J2000.

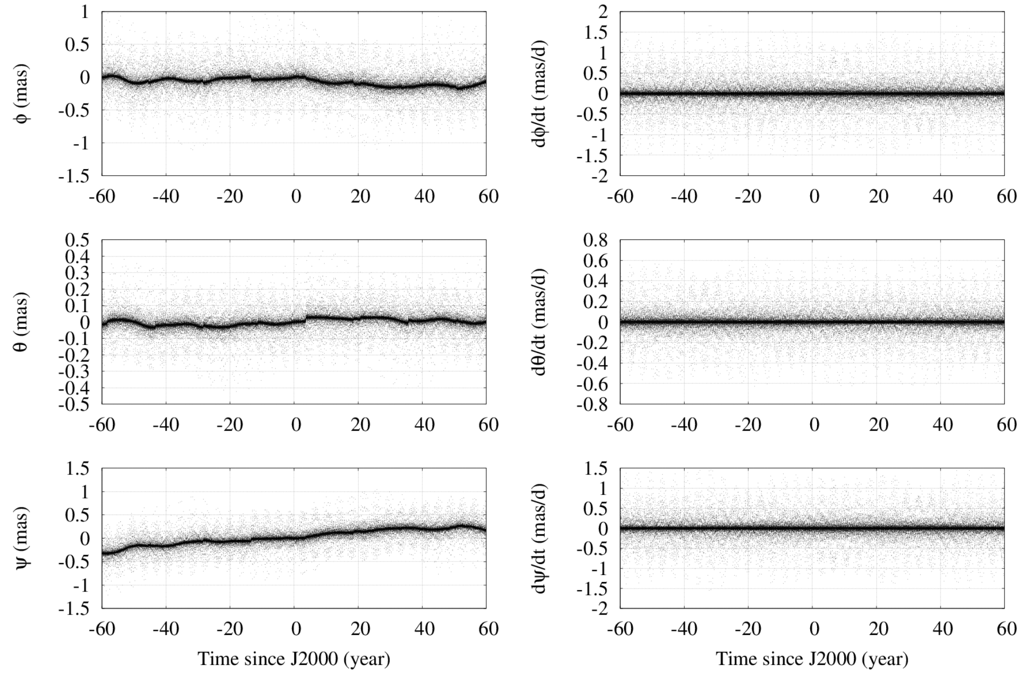

Fig. 3. Differences over the 3 Euler's angles and their time derivatives after an integration with initial conditions provided by INPOP13c. The x axis is TDB time expressed in years since J2000.

5 Conclusion

Our numerical solution of the orbital and rotational motion of the Moon, is very closed to the one of INPOP13c over a time span of 120 years old centred at J2000, as shown with Fig. 1, 2 and 3. The remaining signal on Fig. 1 and 2 is totally explained by the differences of the two modelling (see Sec. 4) while no significant remaining signal is found on Fig. 3. Currently we are fitting our numerical solution to LLR data with the CAROLL reduction software available in POLAC using partial derivatives computed from variational equations.

References

Bertotti, B., Iess, L., & Tortora, P. 2003, Nature, 425, 374

Colladay, D. & Kostelecký, V. A. 1997, Phys. Rev. D, 55, 6760

Colladay, D. & Kostelecký, V. A. 1998, Phys. Rev. D, 58, 116002

Fienga, A., Manche, H., Laskar, J., Gastineau, M., & Verma, A. 2014, ArXiv e-prints

Fischbach, E. & Talmadge, C. L. 1999, The Search for Non-Newtonian Gravity

Hairer, E., Norsett, S. P., & Wanner, G. 1993, Solving Ordinary Differential Equation I. Nonstiff Problems, ed. Springer-Verlag (Springer Series in Computational Mathematics)

Hees, A., Lamine, B., Reynaud, S., et al. 2012, Classical and Quantum Gravity, 29, 235027

Klioner, S. A. & Soffel, M. H. 2000, Physical Review D, 62, 024019

Lambert, S. B. & Le Poncin-Lafitte, C. 2009, A&A, 499, 331

Lambert, S. B. & Le Poncin-Lafitte, C. 2011, Astronomy and Astrophysics, 529, A70+

Merkowitz, S. M. 2010, Living Reviews in Relativity, 13, 7

Müller, J., Williams, J. G., & Turyshev, S. G. 2005, ArXiv General Relativity and Quantum Cosmology e-prints

Soffel, M., Klioner, S., Müller, J., & Biskupek, L. 2008, Physical Review, 78, 024033

Wallace, P. T. 1998, Highlights of Astronomy, 11, 191

Will, C. M. 1993, Theory and Experiment in Gravitational Physics

Williams, J. G., Turyshev, S. G., & Boggs, D. H. 2004, Physical Review Letters, 93, 261101